

Experimental study of factors affecting fault slip rockbursts in deeply buried hard rock tunnels

Fanzhen Meng^{1,2} · Hui Zhou² · Zaiquan Wang¹ · Liming Zhang¹ · Liang Kong¹ · Shaojun Li² · Chuanqing Zhang² · Shanchao Hu³

Received: 9 February 2016 / Accepted: 26 July 2016 / Published online: 12 August 2016
© Springer-Verlag Berlin Heidelberg 2016

Abstract As civil tunnelling and mining have progressed to ever greater depths, the magnitudes of the stresses resulting from these activities have also risen significantly, leading to increasingly frequent excavation-induced seismicity and rockbursts that pose a great threat to workers and equipment on site. Although considerable research effort has been devoted to understanding the factors that influence strain bursts, few studies have addressed the factors affecting fault slip rockbursts triggered by slip on discontinuities such as structural planes. Thus, in the present work, shear tests were performed under constant normal load (CNL) conditions on joints with rough surfaces and interlocked asperities to study their shear behaviour and acoustic emission characteristics. The effects of rock type, normal stress, surface morphology, infilling, and shear history on slip rockbursts were investigated. The test results indicated that slip bursts occur more easily in granite joints because of either sudden and violent post-peak stress drops or stress drops during stick slip. Static shear failure dominated in marble and cement mortar joints, except when the joint surface was extremely

irregular, and rockbursts took place when asperities were sheared off or when tensile ruptures occurred on the joint. The value of the stress drop immediately after peak stress and the value of the average stress drop during stick slip of granite joints both increased with normal stress; thus, the probability and intensity of rockbursts rose with normal stress. The failure modes of the joints were strongly influenced by the normal stress level; fillings and previous shearings (i.e. a shear history) reduce the risk of rockbursts because they reduce the amount energy released.

Keywords Fault slip rockburst · Structural plane · Shear failure · Influencing factor · Acoustic emission (AE)

Introduction

Excavation-induced seismicity and rockbursts are occurring increasingly often as underground tunnelling and mining progress to greater depths. A rockburst is defined as damage to an excavation that occurs in a sudden or violent manner, and it is always associated with a seismic event. In this situation, energy is released: rock blocks may be ejected from the surrounding rock mass, possibly causing significant damage to underground structures and equipment and, most importantly, presenting serious risks to worker safety (Kaiser et al. 1996). A rockburst is considered to be a major geological disaster during the construction of an underground engineering structure. Although extensive research into rockbursts has been conducted and advances have been reported, the mechanics/physics of the underlying processes are far from adequately understood (Ortlepp 2005), so rockbursts remain a hazard (Stacey 2011). Problems with rockbursts have troubled many countries around the world, including South

✉ Fanzhen Meng
xuelianmfzh@163.com

✉ Shanchao Hu
mining2@126.com

¹ College of Science, Qingdao Technological University, Qingdao 266033, Shandong, China

² State Key Laboratory of Geomechanics and Geotechnical Engineering, Institute of Rock and Soil Mechanics, Chinese Academy of Sciences, Wuhan 430071, Hubei, China

³ State Key Laboratory of Mining Disaster Prevention and Control Co-founded by Shandong Province and the Ministry of Science and Technology, Shandong University of Science and Technology, Qingdao 266590, China

Africa, Canada, USA, Australia, and Poland (Ortlepp 2005). With the rapid development of China's national economy, demands on energy sources and infrastructure have also risen sharply, causing the excavation depths of many tunnels to extend beyond 1000 m or even 2000 m, and rockburst hazards have become a significant problem during the construction of deep tunnels in recent years. More than 750 rockbursts occurred during the excavation of seven parallel tunnels in the Jinping II hydropower station under a maximum overburden of 2525 m over an average length of 17.5 km, and the proportions of slight, moderate and (extremely) intense rockbursts were 44.9, 46.3 and 8.8 %, respectively (Feng et al. 2013). An extremely intense rockburst occurred on November 28, 2009, leaving seven workers dead and one injured. Additionally, the tunnel boring machine (TBM) was damaged beyond repair and buried under more than 400 m³ of rock fragments to a distance of approximately 30 m behind the cutter head (Zhang et al. 2012).

Attempts have been made by many researchers to better understand, manage and mitigate rockburst hazards. Various rockburst mechanisms have been proposed and analysed based on laboratory experiments and field investigations to better understand these complex rock-mechanical phenomena (Cook 1965; Hasegawa et al. 1989; Ortlepp and Stacey 1994; Kaiser et al. 1996; Linkov 1996; Ortlepp 2000a; He et al. 2012a; Liu et al. 2013; Cai et al. 2015; Zhou et al. 2015). The various mechanisms that have been proposed by different scholars indicate that rockbursts are complicated phenomena that are initiated under high geostress and brittle rock conditions with extremely complex mechanical features, and they are influenced by the inherent properties of rock, such as its strength and brittleness, and by the external environment, such as the stress state, dynamic disturbance, geological structure and excavation sequence. Thus, much effort has been directed into better understanding the factors that influence rockbursts. Twenty-one rockbursts that caused damage to excavations in deep South African gold mines were investigated, and the principal factors that controlled the severity and distribution of the damage were analysed by Durrheim et al. (1998); it was revealed that the source mechanism was often determined by the mine's layout and by regional structures, such as faults and dykes, and that the local rock conditions and support systems strongly influenced the location and severity of the damage. After analysing the rockburst damage in the Lucky Friday Mine stopes, White and Whyatt (1999) discovered that slip displacements along bedding planes reduced the physical dimensions of the stopes and increased the compressive stress along the stope margins, which promoted the rockbursts. Castro et al. (2009) investigated the influence of unclamping, daylighting, stress rotation and pillar shear on fault slip rockbursts in deep mines via numerical analysis,

and suggested that fault slips may be prevented by pillar clamping and by reasonable stope sequencing. He et al. (2012b) studied the rockburst characteristics of sandstones with bedding planes that are perpendicular or parallel to unloading surfaces using triaxial unloading tests in the laboratory. Huang and Liu (2013) analysed the effect of the loading (unloading) rate and path on the mechanical properties of composed coal rock using uniaxial compression tests, and the rockburst propensities of the composed samples were evaluated. Chen et al. (2014) studied the influence of temperature on rockbursts in granite. The influences of the positional relationship between stopes and faults, the rate of mining, the depth of mining and the friction angle of the fault in fault slip bursts due to ore extraction were investigated numerically by Sainoki and Mitri (2014a). Zhao et al. (2014) investigated the influence of the unloading rate on strain bursts in granite under true triaxial unloading conditions and found that the rock samples were prone to strain burst failure under a high unloading rate, while nonviolent spalling occurred under a low unloading rate. The experimental results by Zhao and Cai (2015) indicated that the height-to-width (H/W) ratio of rock specimens affected the behaviour of strain bursts.

Two classes of rockbursts in deep mines were classified by Ryder (1988): class C (crush/collapse) events and class S (slip/shear) events. Ortlepp and Stacey (1994) suggested five source mechanisms for rockbursts: strain bursts, buckling, face crushing, virgin shear and reactivated shear on existing faults or discontinuities. The authors noted that the last two shear mechanisms were likely to occur in large-scale mining operations. Kaiser and Cai (2012) grouped buckling-type bursts with strain bursts and shear rupture-type bursts with fault-slip bursts, forming three generalised types of rockbursts: strain bursts, pillar bursts and fault-slip bursts. Based on the roles that small-scale structural planes played in rockbursts in civil tunnels with deep, hard rock, rockbursts were classified into fault-slip bursts and shear rupture bursts (triggered by slip along structural planes) and into buckling bursts (caused by the compression failure of rock plates separated by structural planes) (Zhou et al. 2015; Meng et al. 2016). According to the aforementioned rockburst classification method, rockbursts can be grouped into two broad categories based on the failure mechanism involved. The first group is mainly caused by compression failure of wall rocks, such as strain bursts, face crushing, pillar bursts and buckling bursts, whereas the other group is induced by shear failure along discontinuities such as large faults (tens to hundreds of metres long) in deep mines or small structural planes (from less than one to a few metres long) in civil tunnels of deep, hard rock. Seismic events induced by shear failure of rock masses or fault reactivation have magnitudes of >2.5 ; indeed, the magnitude occasionally exceeds 4.0 (Hofmann and Scheepers 2011; Alber 2013), resulting in devastating

damage to mine openings in a large area of an underground mine. Therefore, many researchers have investigated the evolution process, source parameters and the potential for fault slip rockbursts by microseismic monitoring and numerical modelling (Ryder 1988; Morrison 1989; Swanson 1992; Simon 1999; Ortlepp 2000b; Hofmann and Scheepers 2011; Vatcher 2012; Sainoki and Mitri 2014a, 2015).

A summary of the different rockburst types based on the mechanism (compression or shear failure) is listed in Table 1. The table shows that strain bursts, face crushing and pillar bursts are all caused by the violent fracture of intact rock under a compressive load in the sidewall, workface and rock/mine pillars, and can be regarded as generalised strain bursts. Most of the aforementioned studies regarding the factors influencing rockbursts concentrated on this type of burst. Compared to the numerous studies of the factors influencing strain bursts, studies of the factors that affect bursts caused by the movement of pre-existing faults/structural planes or by the formation of seismically active structural zones are rather scarce. Rockbursts that are triggered by slip along discontinuities in deep, hard rock tunnels can cause great damage to facilities, workers and underground opening stability. For example, the extremely intense rockburst at Jinping on November 28, 2009 was related to the slip of a rigid structural plane, and caused seven deaths and the total destruction of the costly TBM machine. When the plane was about to slide, the shear deformation intensified, which increased the deformation potential and in turn led to the release of more energy. The failure zone of this burst is shown in Fig. 1. Moreover, shear tests should be performed in addition to compression tests to study the factors influencing these shear-type bursts.

The work reported in this paper was primarily performed to study the factors that influence fault slip rockbursts in deeply buried hard rock tunnels. Completely locked joint specimens were created to simulate the rigid structural planes in deep tunnels, and shear tests under constant normal load (CNL) conditions were conducted. Acoustic emission (AE) signals during shearing were also recorded. The shear behaviour and acoustic emission characteristics were

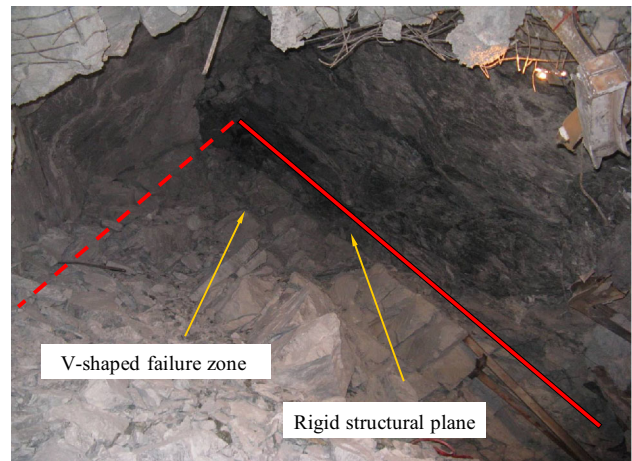


Fig. 1 V-shaped failure zone and exposed structural plane after the extremely intense Jinping rock burst on November 28, 2009 (Zhang et al. 2012; Zhou et al. 2015)

analysed, and the influences of rock type, normal stress, surface morphology, infilling and shear history on fault slip rockbursts were investigated. The experimental results of this study enhance our mechanistic understanding of factors that can influence rockbursts triggered by slip along discontinuities in deep hard-rock tunnels.

Shear tests of different rock joints

Joint sample preparation

To study the mechanical behaviour of different rock types, two hard rock types (granite and marble) that are commonly encountered during the construction of deep civil tunnels and one rock-like material consisting of cement mortar were selected for comparison. High-strength cement, fine quartz sand and water were mixed in a ratio of 1:1:0.5 by weight and poured into a mould with dimensions of 50 cm × 40 cm × 12 cm, followed by compaction to get rid of the bubbles. The cement mortar was left undisturbed for 1 day before removing the mould. This specimen was cured at room temperature for 1 month and was

Table 1 Generalized classification of rockbursts based on the failure mechanism

Condition of the rock mass	Failure mechanism	
	Compression-dominated	Shear-dominated
Intact surrounding rock	Strain burst Pillar burst Face crushing	Shear rupture burst
With discontinuities	Buckling burst	Fault slip rockburst ^a

^a In deep mines, it is the reactivation of large-scale faults (tens to hundreds of metres long) that causes a fault slip rockburst, while in deep civil tunnels (traffic tunnels or headrace tunnels), the activation of small-scale structural planes (from less than 1 m to a few metres long) triggers a fault slip rockburst

then cut with a saw into cubic samples with dimensions of 10 cm × 10 cm. Cubic samples 10 cm on a side were cut from a long piece of granite collected from a building material market and then ground to make the opposite faces parallel according to the suggested method of the International Society for Rock Mechanics (ISRM). Marble was sampled from the Jinping II hydropower station and processed using the same method and standard as granite. The

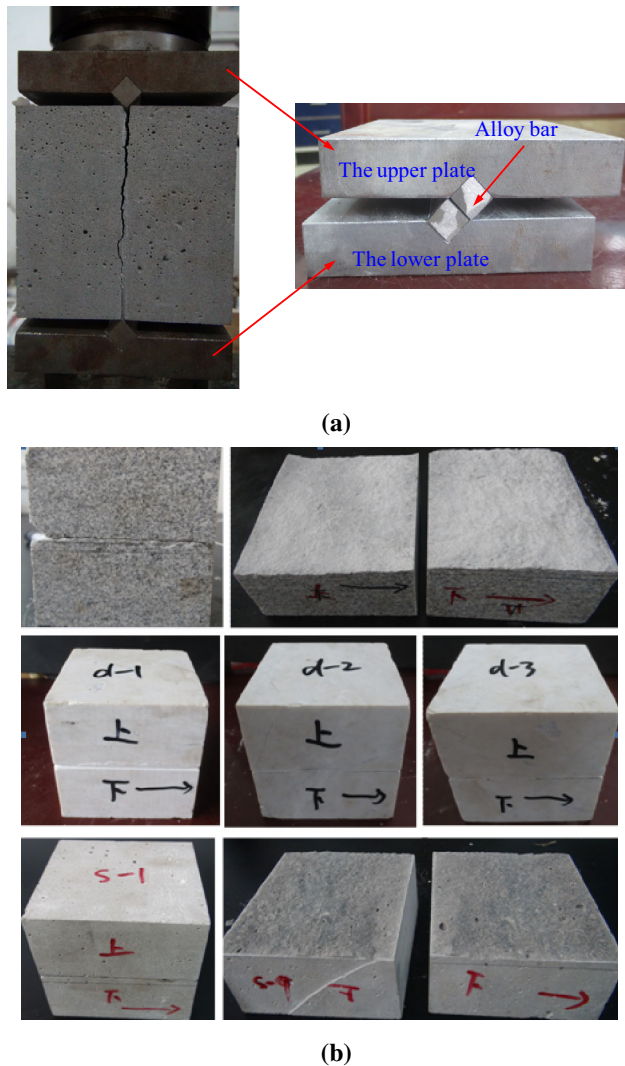


Fig. 2 **a** Splitting mould that was used in the experiment, and **b** some of the split joint samples (from top to bottom: granite joints, marble joints and cement mortar joints)

Table 2 Basic mechanical parameters and normal stresses for the three different types of joints that were applied in the shear tests

Type of joint	σ_c (MPa)	E (GPa)	μ	Normal stresses (MPa)
Cement mortar	46.39	7.28	0.077	0.5, 1, 2, 3, 4, 5, 7, 10, 14, 20
Granite	191.24	20.74	0.132	1, 3, 5, 7, 10, 20, 30, 40, 45
Marble	95.27	17.56	0.074	1, 3, 5, 7, 10, 15, 20, 30, 40

σ_c , E and μ are the uniaxial compression strength, elastic modulus and Poisson ratio, respectively

basic mechanical parameters of the three different types of rock are listed in Table 2.

A field investigation in the Jinping II intake tunnels showed that several high-intensity rockbursts took place when shear failure occurred along tightly interlocked structural planes that concentrated a great deal of energy (the weak planes also offered additional degrees of freedom during failure); thus, a special mould similar to that used in Brazilian disk splitting tests was designed to split cubic specimens (with 10 cm long sides), and joints with rough surfaces and interlocked asperities were created. The splitting mould and the prepared joint samples are shown in Fig. 2.

Experimental system and methods

Shear tests were performed at the Institute of Rock and Soil Mechanics, Chinese Academy of Sciences, using an RMT150C testing machine; such machines have been widely used by other researchers (Zhou et al. 2015). Normal stress was applied via the adjustable vertical piston, and shear stress was applied through a horizontal hydraulic jack, which drives two horizontal dowels by pulling on the lower shear box. The maximum normal and shear load values were 1000 and 500 kN, respectively. During the tests, a normal load was applied at a rate of 1 kN/s, and after a predetermined normal load value was reached, the shear load was subsequently applied at a rate of 0.005 mm/s with the normal load remaining constant.

Because rockbursts are violent expulsions of rock under high-geostress conditions, and the burst occurrence frequency and intensity are closely related to burial depth, normal stresses ranging from 0.5 to 45 MPa were exerted to study the mechanical behaviours of joints under different stresses (especially under high normal stress) and the effects of normal stress on fault slip rockbursts. The normal stresses applied to the three different joints during the shear tests are also detailed in Table 2.

The same amounts of dry soil (with a water content of 4.96 %), wet soil (with a water content of 29.15 %) and cement mortar particles were filled between the cement mortar joint surfaces to investigate the effects of different infillings on the shear behaviour of joints and to determine the influence of infillings on fault slip rockbursts. This is discussed in detail in Sect. 3.4.

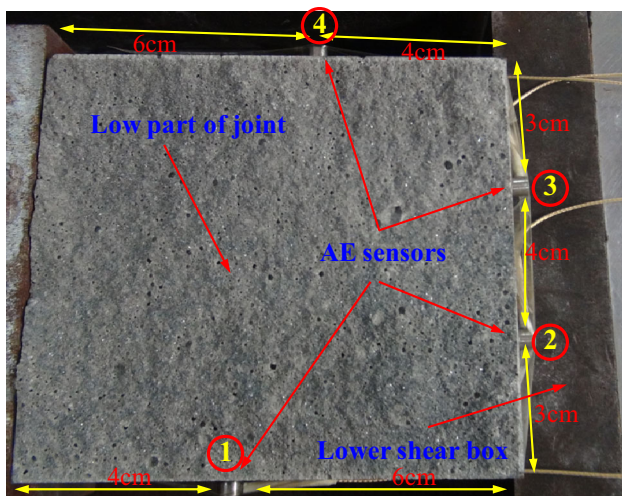


Fig. 3 Arrangement of the AE sensors (the four sensors were within the same plane, which was 0.5 cm from the surface; the numbers in circles are number labels for the sensors)

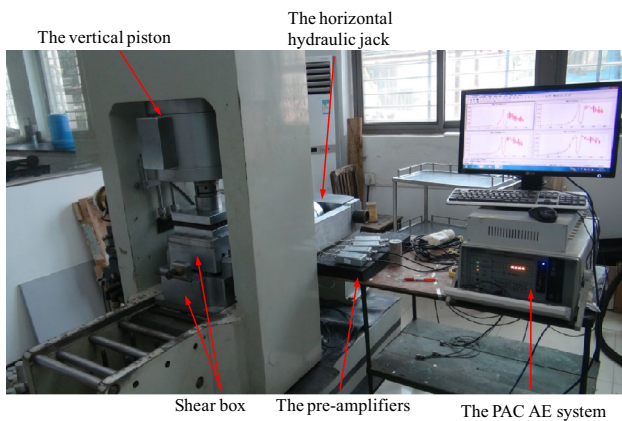


Fig. 4 Image of the setup during the shear experiment

Acoustic emissions were monitored with a 16-channel PAC-DISP system, and four PICO sensors 5 mm in diameter and 4 mm in height were attached to each side of the low part of the joint in a plane. A layer of couplant was painted onto the interface of the rock and the piezoelectric ceramic of the sensor. The arrangement of the sensors is shown in Fig. 3. The resonant frequency and operating frequency range of the sensors were 500 and 200–750 kHz, respectively, and the sampling rate was set to 1 million samples per second. The amplification of the preamplifier and the threshold of the system were both 40 dB. To ensure that the shearing process was synchronised with the acquisition process of the AE, the AE system was triggered simultaneously when shear stress was applied. An image taken during the shear experiment is shown in Fig. 4.

Analysis of the factors influencing fault slip rockbursts

The shear stress vs. shear displacement curves of the cement mortar joints, marble joints and granite joints are shown in Fig. 5. In general, the shear stress of the cement mortar under different stresses varied in a stable state with shear displacement, as shown in Fig. 5a, and no noises were emitted except when the normal stress was 4 MPa; this situation will be discussed in Sect. 3.3. When the normal stress was higher than 10 MPa, the stress curves during the post-peak period were not smooth and showed some fluctuation. For the marble joints, the shear stress increased gradually to the peak value and then decreased slowly to the ultimate shear strength with shear displacement, and the stress curves are characterised by smoothness and by inconspicuous displacement weakening regardless of whether the normal stress was low or high, as shown in Fig. 5b; one exception emerged when the normal stress was 3 MPa, which will be discussed later. Shear stress curves of granite joints are illustrated in Fig. 5c, and it can be seen that the granite joints show strong brittle failure characteristics with increasing normal stress. A violent post-peak stress drop occurred when the normal stress was higher than 5 MPa, and then the shear stress increased again with shear displacement to a relative peak value and subsequently decreased to the ultimate shear strength. Unstable stick slip, which is defined as a spontaneous jerking motion that occurs while two objects are sliding over each other, appeared when the normal stress was higher than 10 MPa. During the process of stick slip, continuous noises were generated and transmitted from the shear boxes, and every small stress drop corresponded to a very loud sound, indicating that enormous energy was being released.

From the above analysis, we know that the shear behaviour varies for different rock types and different normal stress states, which may have different effects on fault slip rockbursts. The in situ investigation of the failure modes of structural planes in the deep tunnels of Jinping II hydropower station suggests that not all of the shear failures along structural planes in the vicinity of the tunnels could have led to dynamic rockbursts; most of these failures occurred in static mode. Therefore, it is important to determine the factors that determine the shear failure mode (static or dynamic) of a structural plane. In the following sections, factors such as rock type, normal stress, and other factors that influence fault slip rockburst are analysed in detail based on the shear test results and the monitored acoustic emission.

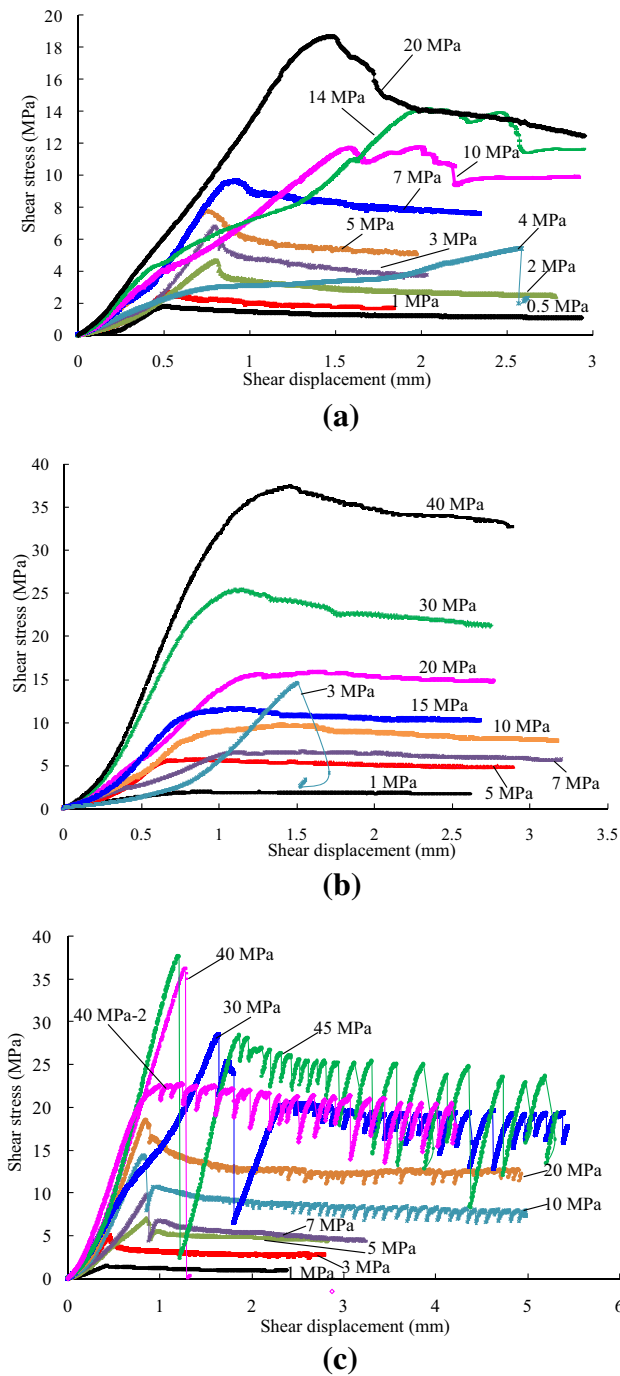


Fig. 5 Curves of shear stress vs. shear displacement for cement mortar joints (a), marble joints (b) and granite joints (c) (as the peak stress dropped to 0 from 36 MPa for the granite joint when the normal stress was 40 MPa, the loud sound that was emitted made the experimenter think that something was wrong with the test system, so the experiment was stopped; the 40 MPa-2 curve is the curve for the same joint after a second shearing)

Rock types

A comparison shows that shear failure of the granite joints proceeded in violent stress drops after the peak shear stress

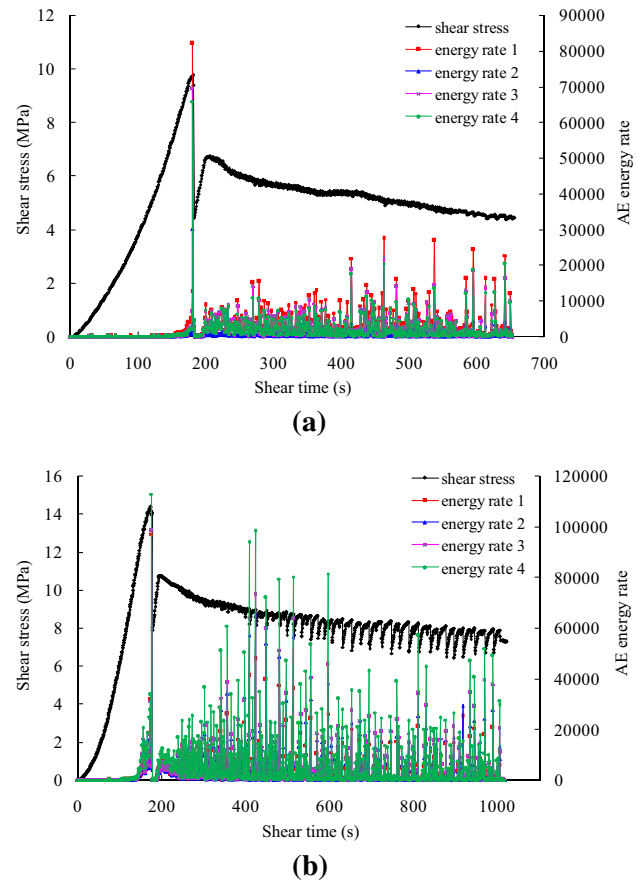


Fig. 6 Change in the AE energy rate with shear time for granite joints under a normal stress of a 7 MPa or b 10 MPa

was reached under a certain value of normal stress (Fig. 5c shows that the post-peak stress drop occurred when the normal stress was >5 MPa). A relatively high amount of energy and a loud sound were released at this moment, with the amount of energy released reaching its maximum throughout the entire shear process. By performing dynamic analysis using Barton's shear strength criterion, Sainoki and Mitri (2014b) found that fault slip rockbursts can be induced by a stress drop resulting from asperity shear, and the magnitude of the fault slip and seismically radiated energy increases with increasing fault surface roughness. This study indicates that the stress drop plays a decisive role in triggering the fault slip burst.

The changes in energy rate with shear time for granite joints under 7 and 10 MPa of normal stress are demonstrated in Fig. 6a, b, respectively. Energy rates 1, 2, 3 and 4 in the graphs indicate the AE energies that were recorded by the first, second, third and fourth sensors, respectively, in 1 s. The AE energy is defined as the area enclosed by the signal envelope (in mV) and the abscissa (in μ s) in mV μ s. Moreover, the shearing of the granite joints was characterised by unstable stick slip under certain pressures (from 10 to 45 MPa in this experiment), which was not seen for

the other two joint types. The energy increased to a relative maximum value (usually higher than 1×10^4) at small stress drops, and was accompanied by loud sounds, as shown in Fig. 6b.

Thus, the violent stress drops that occur immediately after the peak shear stress and the periodic small stress drops that occur during the stick-slip period may cause rockbursts because of the great amount of energy released, and there are two possible locations for the damage. In the first, the slippage zone is coincident with the damage location, i.e. the shear failure of the structural plane itself is a rockburst, and the rock mass on the hanging wall or footwall (the part that will slide depends on the orientation of the principal stress applied on the plane; Zhou et al. 2015) is ejected by the released energy. The other possibility is that the shear failure itself is not the rockburst site, e.g. the structural plane is located in the internal rock mass slightly away from the side wall of the tunnel. The released energy acts as a seismic wave which is transmitted through the rock mass to these unravelling and bulking rocks or to intact rock around the tunnel under a critical stress state, and so rock erupts out with kinetic energy under the influence of static stress coupled with dynamic stress (seismic waves). In this case, the seismic origin does not coincide with the damage zone of the burst. Moreover, rockbursts may occur repeatedly at the site if unstable stick slip occurs because of intermittent and periodical energy release.

Compared with the strong post-peak stress drop and the jerky unstable slip (stick slip) noted for granite joints, the shear failure processes of the marble and cement mortar joints were quieter and slower. The peak shear stress decreased very slowly rather than decreasing dramatically with displacement, and the amount of energy that was released was much less than that in the granite joints (the energy rate curves for the cement mortar joint under 10 MPa of normal stress and the marble joint under 40 MPa of normal stress are shown in Fig. 7a, b, and the peak energy rates for the two types of joint were in the range 10^2 – 10^3 ; few values exceeded 10^4), indicating a low probability of rockbursts. There were two exceptions for the cement mortar and marble joints under a normal stress of 4 and 3 MPa, respectively, where shear failure occurred through stress drops, which will be discussed in Sect. 3.3. However, when the structural plane around the tunnel shears under thrust, the hanging wall or footwall slides towards the excavation and squeezes the surrounding rock, which makes the rock more compressed. Stress is concentrated and energy builds up continuously, and rockbursts may also occur when the concentration reaches a certain level. In summary, shear failures of granite joints under high normal stresses are more prone to rockbursts (the plane itself is also the damage site or acts as the

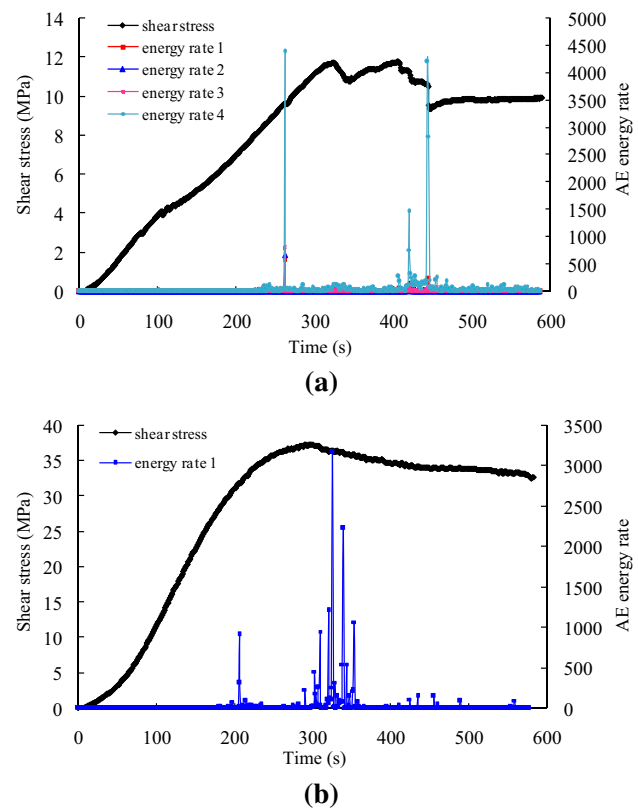


Fig. 7 Change in the AE energy rate with shear time for a cement mortar joint under 10 MPa of normal stress (a) and a marble joint under 40 MPa of normal stress (b)

seismic focus that emits seismic energy), while the possibility of fault slip rockbursts is low for cement mortar and marble joints. However, rockbursts may occur in rock-masses with weak brittle failure characteristics because of movement along the plane, which elevates the compressive stress concentration.

Normal stresses

The stress state usually has a decisive effect on rock failure. For jointed rock masses, rocks on one part will slide over the asperities on the opposite part under low normal stress, and dilatancy occurs; under high normal stress, the rough asperities are sheared off directly, and the dilatancy effect is weakened.

The shear test results revealed that the shear behaviour of the granite joints was the most heavily affected by normal stress. Once dilation was prevented under high normal stress, granite built up substantial apparent cohesion and thus failed differently at elevated normal stress than seen for the other two weak rock types (which had little or no apparent cohesion). Three stages could be distinguished according to the shear characteristics with increasing normal stress. (1) Static shear failure occurred at

a relatively low normal stress (<3 MPa). (2) A post-peak shear stress drop occurred when the normal stress was >5 MPa, and the value of the stress drop (the difference between the peak shear stress and the stress at the terminal point of its decline) tended to increase with normal stress, as shown in Fig. 8a. (3) A post-peak shear stress drop and stick slip occurred simultaneously at a relatively high normal stress (>10 MPa in this test). The change in the average stress drop with normal stress, which was calculated by dividing the total number of oscillations by the sum of each stress drop value during stick slip, is demonstrated in Fig. 8c. The mean amplitude of the stick slip also increased with normal stress, and the amplitude at the beginning of the jerky motion was small and gradually grew with each cycle, as shown in Fig. 8b. For the granite joints, the risk of fault slip rockbursts increased with the stress state: ordinary static shear failure dominated at lower normal stresses, and dynamic shear failure with enormous energy release occurred at higher normal stresses. The intensity of the rockbursts also rose with normal stress.

The failure mode and pattern of the granite joints were also influenced by the magnitude of the normal stress. Viewed externally, the joint specimen appeared to remain relatively intact except for a small narrow region along the front of the hanging wall which fractured under low-stress conditions. The surfaces of these joints were worn to some degree; no other fractures were generated in the specimen. Images that were taken after shearing when the normal stress was 1 MPa are shown in Fig. 9; the arrow in the footwall indicates the shear direction. The damage on the surface was aggravated with increasing normal stress, and tensile failure emerged on the footwall or hanging wall in addition to damage to the asperities and impact fractures along the front end. An image of the specimen after shearing when the normal stress was 40 MPa is shown in Fig. 10; the trend of these tensile fissures intersects with the horizontal shear direction at an acute angle.

For the cement mortar joints, the failure patterns were also affected by the normal stress, although the shear failures for most of the joints were static. Except for slight abrasion on the joint surface, the two parts of the joints were unbroken under low normal stress. As the normal stress increased, the front end of the hanging wall was shocked out and left on the footwall; as the normal stress continued to increase, many more tensile fractures started to appear in the footwall and hanging wall, intersecting with the shear direction at an acute angle, as shown in Fig. 11. The level of the normal stress had a similar effect on the marble joints, and Fig. 12 shows an image of the footwall after failure under 40 MPa of normal stress. The surface of the joint was quite flat, and long, narrow debris remained on the footwall after shear. Additionally, three long cracks propagated to the bottom of the footwall. From

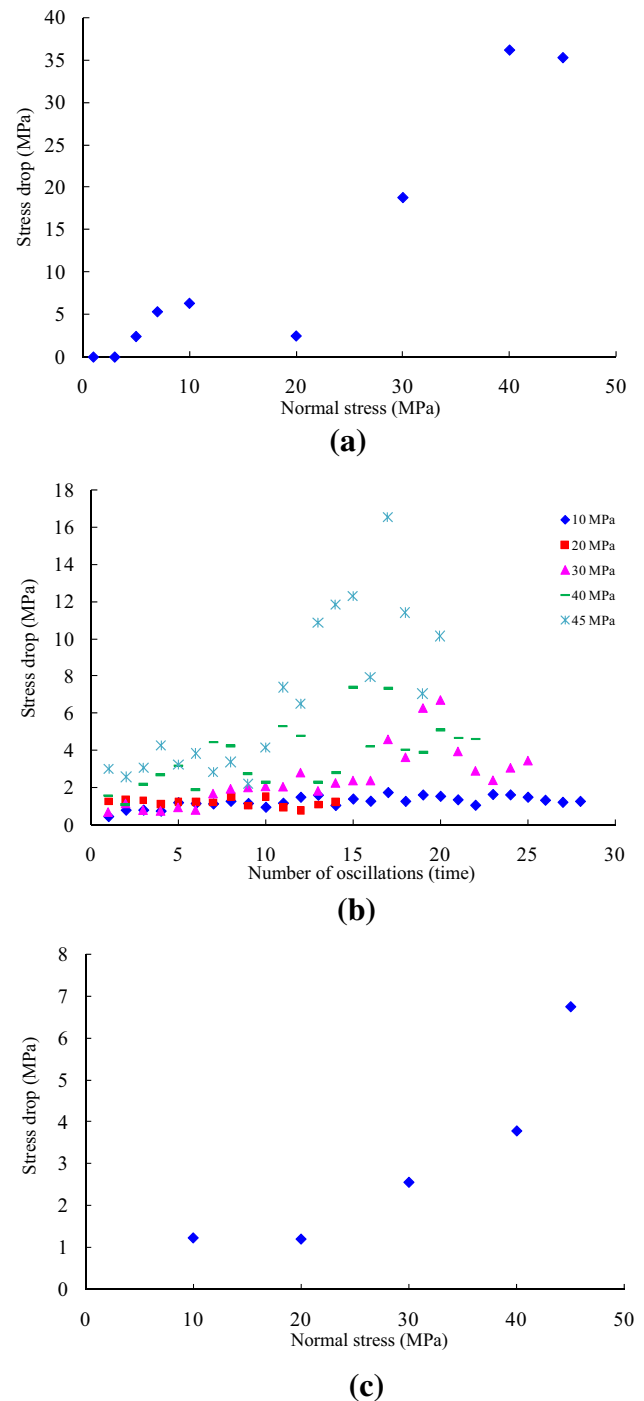
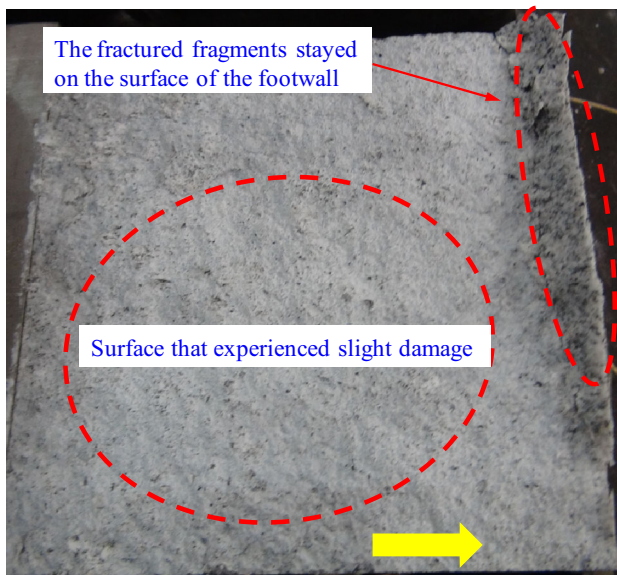
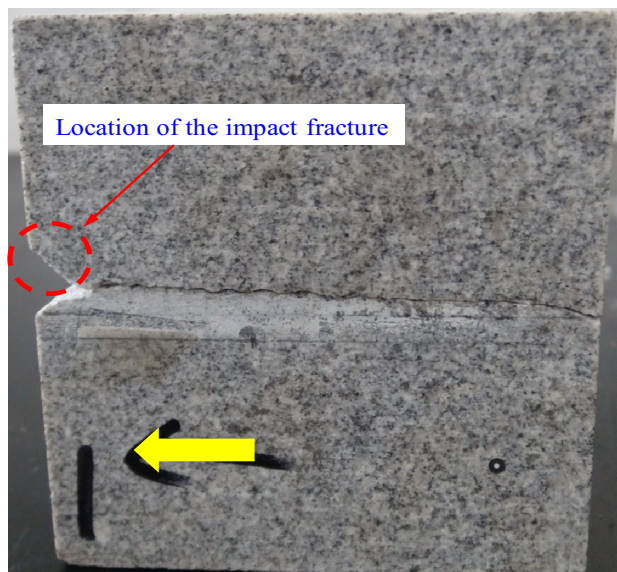


Fig. 8 Change patterns of the stress drop for granite joints: **a** change in the first violent stress drop with normal stress; **b** evolution of each stress drop during stick slip with the number of cycles; **c** change in the average stress drop at a given normal stress during stick slip. (Because the test was stopped after the violent stress drop when the normal stress was 40 MPa, the stress drops for this normal stress were the result of the second shearing of the same joint)

Figs. 10, 11 and 12, we know that the three different types of joints presented very similar appearances after shear failure when the normal stress was high (relative to the



(a)



(b)

Fig. 9 Images after shearing of granite joints under 1 MPa of normal stress (the *arrow* shows the shear direction, and the hanging wall was motionless during shearing): **a** is the surface of the footwall and **b** is the locked footwall and hanging wall

compression strength of the material): asperity damage and breakage as a result of attrition on the surface, impact fractures at the boundaries of the joints perpendicular to the shear direction, and tensile fissures on the footwall that were connected with the surface plane at an acute angle. The main difference between them is the energy released during the failure process. If enough energy is liberated, which is the case for granite joints, then the impacted debris and thin rock plates separated by tensile cracks may be expelled violently, so the fragments after the rockburst are characterised by blocky and slabby structures—

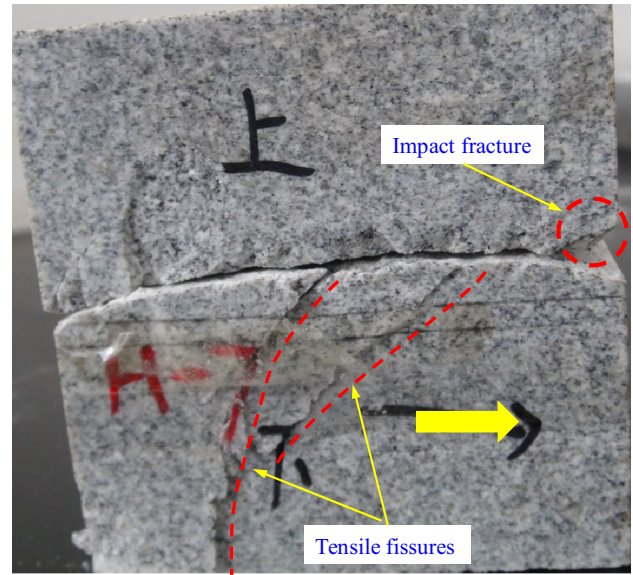


Fig. 10 Failure modes of a granite joint under 40 MPa of normal stress

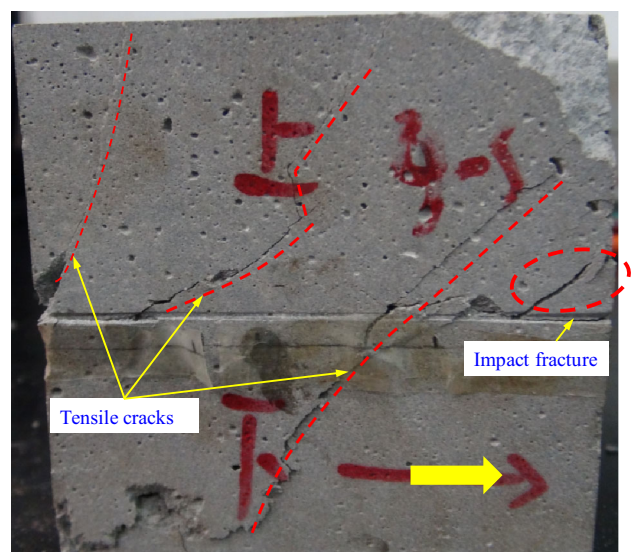


Fig. 11 Image of the failure patterns of a cement mortar joint after shearing under 14 MPa of normal stress

consistent with the extremely intense rockburst in Jinping II's deep tunnels on November 28, 2009 (Zhang et al. 2012; Zhou et al. 2015). To study the failure mechanisms of structural planes, shear tests on irregular artificial saw-tooth joints with different asperity heights were performed by Zhou et al. (2015). Three failure mechanisms were revealed by Zhou et al. (2015) and were also observed in the present study. However, some significant differences were discovered when a comparison was made between the two studies. Impact fractures and tensile failure started to appear under relatively low normal loads in the former study (50 kN or 2 MPa); however, in the present study,

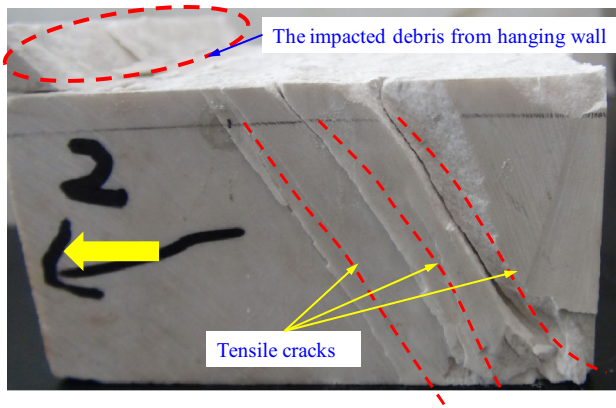


Fig. 12 Image of the failure modes of a marble joint after shearing under 40 MPa of normal stress

impact fractures emerged under intermittently high normal loads, and tensile cracks were only found under relatively high normal loads. The different responses to normal stress in the two studies stem from the different joints that were used. The saw-toothed asperities on the joint surfaces in the study by Zhou et al. (2015) were much rougher than those made by artificial splitting, and the tensile stress was concentrated in the wave trough, which caused cracks to initiate and propagate easily when the tensile strength of the material was exceeded. Moreover, as the row of tooth on the leading end of the hanging wall can hinder the forward movement of the footwall when the slide occurs, it will be shocked outward by friction and the instantaneous release of energy. However, the surfaces of most splitting joints are rather flat compared to serrated joints; the friction (determined by the normal load) has to reach a certain level before the front end of the hanging wall is expelled out. Concentrated tensile stress was difficult to generate on small asperities on the planar surface under low normal stress; only when the normal stress increased to a certain level did the high friction between the sliding surfaces lead to tensile failure, which was initiated from the appressed contact points in the bodies of the two parts. Thus, it is the size and morphology of the asperities on the joint surface that caused the different failure patterns and responses to normal stress. The most common shear failure modes of joints are the overriding of asperities under low stress levels and asperity breakage under high stress levels. Tensile fissures on the hanging walls and footwalls of joints have only rarely been reported in previous studies, except by Zhou et al. (2015), because of the small normal stress applied. This finding is of vital importance to understanding and explaining rockbursts caused by shear failure along structural planes under high-stress conditions in deep hard-rock tunnels.

Surface morphology

The surface morphology of a completely interlocked joint plays an essential role in controlling the mechanical behaviour of the joint, and may influence the occurrence of fault slip rockbursts. The aforementioned cement mortar joints under 4 MPa of normal stress and marble joints under 3 MPa of normal stress were examined to determine the influence of morphology or roughness on rockbursts.

The shear stress curve of the cement mortar joints with 4 MPa of normal stress differed markedly from the others, as shown in Fig. 5a. Before the peak shear stress, a large deformation appeared, and then the peak stress suddenly dropped to a low value, which has only rarely been observed in experimental studies of cement mortar joints, so it is necessary to examine the underlying reasons.

Figure 13 presents a comparison of the hanging wall and footwall of the joint before and after shearing, and shows that the joint surface was extremely irregular and uneven. The cleavage plane was expected to split along the horizontal groove on the side of the footwall. However, the actual fracture face greatly deviated from the pre-designed location, making the joint surface extremely bumpy. In addition to the asperity damage, tensile cracks which initiated from the valleys between the asperities were also generated on the footwall and hanging wall. Tensile fissures generally started to appear when the normal stress was >10 MPa for the cement mortar joints, but stretching cracks arose earlier than anticipated when the normal stress was 4 MPa, which can be attributed to the rough asperities that made it easier for the tensile stress to concentrate and accumulate more easily.

The energy and hit rate that were recorded by sensor 1 for this joint during shearing are shown in Fig. 14. The two parameters increased dramatically at the stress drop, and the energy rate rose to 1.4×10^4 , indicating that a large

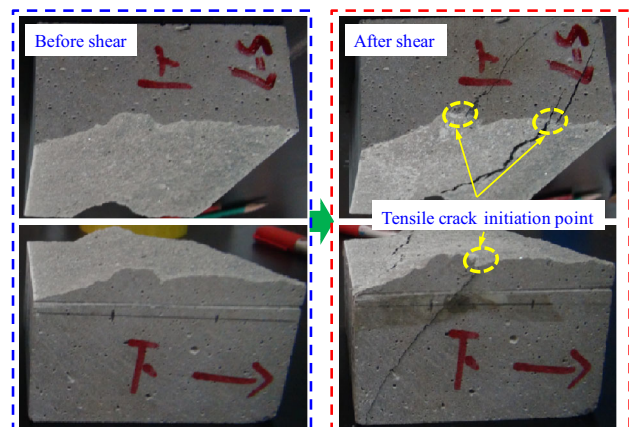


Fig. 13 Comparisons of cement mortar joints under 4 MPa of normal stress before and after shearing

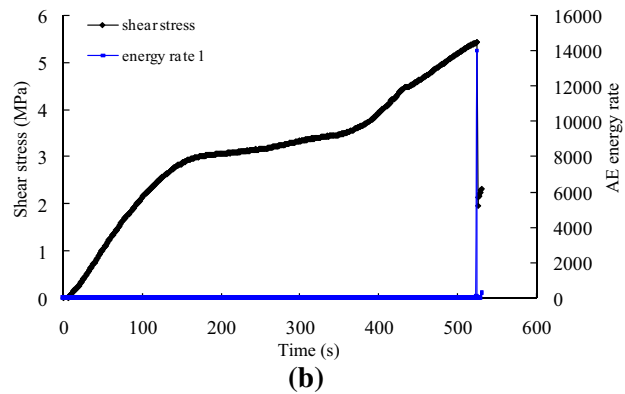
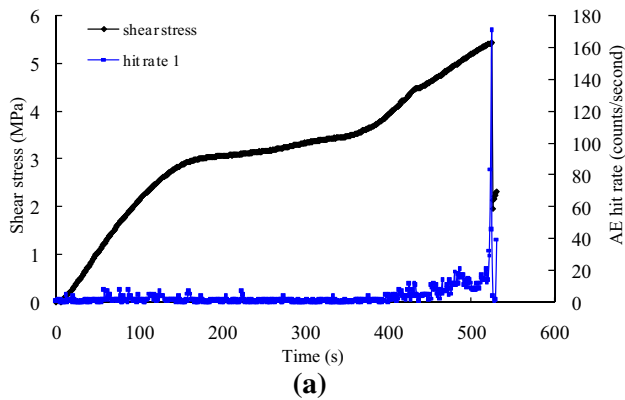


Fig. 14 Changes in the AE hit rate (a) and energy rate (b) with shear time for cement mortar joints under 4 MPa of normal stress

amount of energy was liberated when failure occurred. This finding shows that dynamic shear failure may occur for cement mortar joints when the surface is extremely rough and asperities are large, even when the normal stress is not extremely high.

The shear stress of the marble joints under 3 MPa of normal stress also behaved differently from the curves in Fig. 5b. An image of the joint before shearing is shown in Fig. 15. The green solid line, the red hidden line and the yellow dotted line signify the positions of the expected splitting surface, the actual splitting surface and the actual shear failure plane, respectively, and the arrow indicates the shear direction. The joint was not sheared along the splitting surface (which greatly deviates from the expected cleavage plane) but was sheared primarily in the intact rock, and a new failure plane was formed, leaving the original splitting joint surface undamaged. Figure 5b shows that the shear strength was nearly equal to that of the joint under 20 MPa of normal stress, and that a violent post-peak stress drop occurred due to the shearing off of an intact rock specimen rather than shearing along the weak joint. The changes in the energy rate and shear stress with time are shown in Fig. 16, which shows that the energy jumped to nearly 1.2×10^4 when failure occurred, and a large bang was heard simultaneously (the shear stress graphs in Figs. 5b

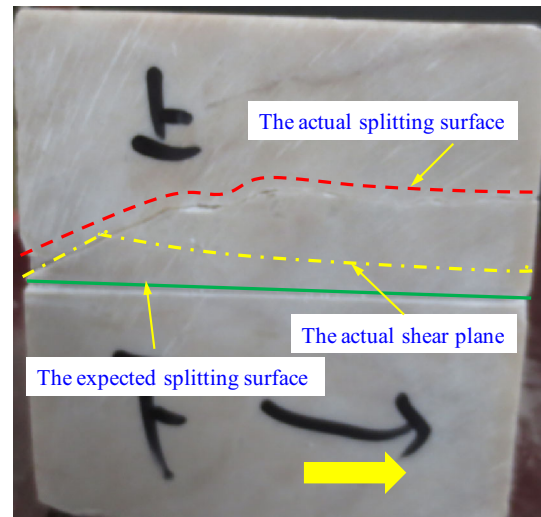


Fig. 15 Image of a marble joint before shear when the normal stress was 3 MPa; the actual splitting surface and shear plane are marked in the picture

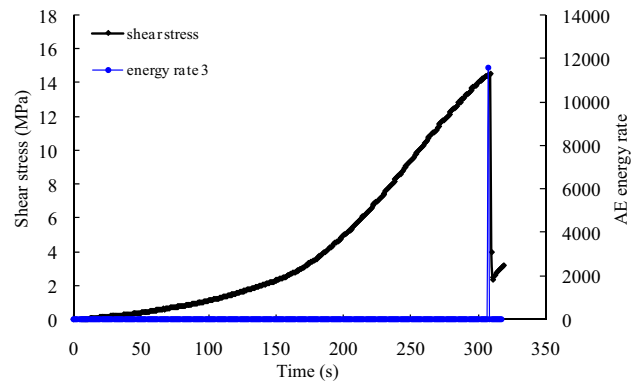


Fig. 16 Change in the AE energy rate with shear time for marble joints when the normal load was 3 MPa

and 16 differ because the abscissae are the shear displacement and time, respectively). This type of shear failure can lead to shear rupture bursts in deep hard-rock tunnels, and the intensity of these bursts may be higher than those caused by weak joint slips under similar stress conditions.

For the granite joints, the influence of normal stress on the shear behaviour and on rockbursts was more obvious than that of the surface morphology because energetic stress drops and unstable stick slip can occur as long as the normal load reaches a certain level for both rough and planar surfaces. However, this finding does not imply that the morphology or roughness does not influence the mechanical behaviour of the granite joints. The conclusions that were obtained from the cement mortar and marble joints regarding the effect of surface morphology also apply to the granite joints, and a rougher surface will lead to more violent brittle failure under the same normal stress conditions.

Infillings

Discontinuities such as fault planes, joints and bedding planes in underground rock engineering may be filled with different types of materials such as clay minerals, rock fragments and soil debris, and it is well known that the infillings will be sheared, and that the shear strength of jointed rock masses is determined by the strength of the infillings if the interlayer is thick. However, the mechanical properties of joints filled with a small quantity of material are not fully understood, and the influence of infillings on fault slip rockbursts needs to be studied. In the cement mortar joint shear tests, a bottle cap of dry soil, wet soil and cement mortar particles from a previously broken specimen were used as infillings to investigate the shear behaviours of three carefully selected joints with relatively planar surfaces under the same 3 MPa normal stress.

Three joints with different infillings before and after shearing are presented in Fig. 17. The dry soil grains were crushed, and some small white regions that were created by the contact and sliding of convex asperities after penetrating the soil layer were distributed on the surface, indicating that the shear medium of the joint that was covered by a handful of dry soil was soil particles and the raised asperities. Fewer asperities were damaged and the surface of the joint was in better condition for the joints with wet soil infillings than for the joints that were filled with dry soil. The white regions were almost invisible, and the wet soil became a layer of thin skin under squeezing and friction. In the joints that were filled with cement mortar particles, some of the granules remained intact and were not crushed because of the low normal stress; thus, the actual shearing medium was these large scattered particles

and the joint surface (point-face friction), and the two opposite joint faces were not touched.

Figure 18 shows the shear stress vs. shear displacement curves for unfilled and filled joints under 3 MPa of normal stress. The graphs show that the shear strength of the infilled joints was dramatically lower than that of the fully interlocked joints with no infilling. No displacement weakening occurred, and the shear stress remained nearly constant after the peak stress was reached. The bare joints had the highest shear strength, followed by the joints that were filled with dry soil, cement particles and wet soil.

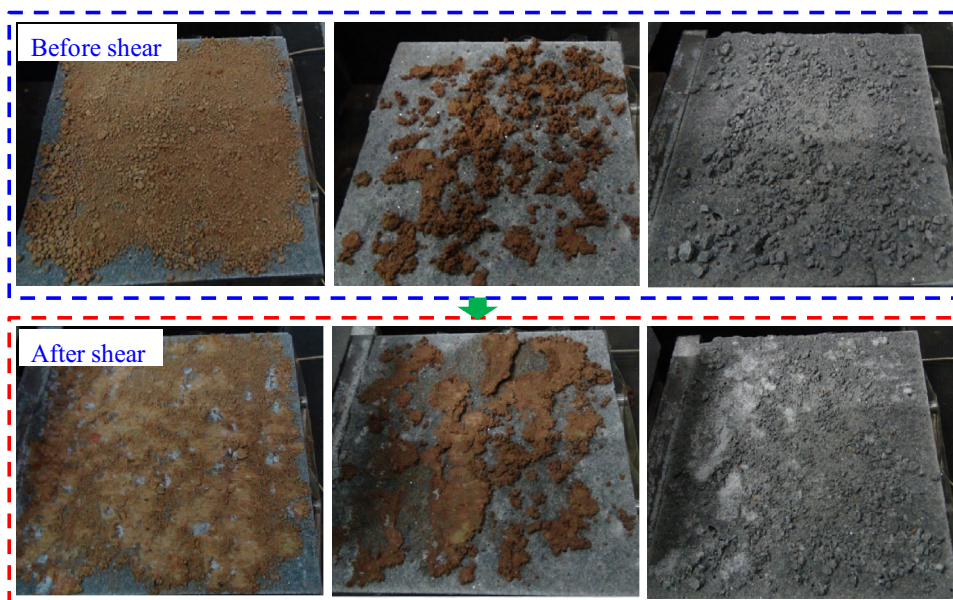
Because the peak shear strength decreased significantly when the joints were filled with materials such as those from our experiment (soil, clay and rock debris), and because the shear stress did not drop any further with increasing shear displacement, the energy that was released was greatly reduced, as verified by the monitored AE energy rate (illustrated in Fig. 19). A comparison of the energy rates from joints without fillings and joints that were filled with dry soil shows that the risk of fault slip rockburst for the filled joint was extremely low or absent because of the extremely low energy release.

Shear history

To study the effects of shear history on the mechanical behaviour of joints and rockbursts, some of the joints were sheared twice or three times under the same normal stress at the same shear rate. The results for the cement mortar and granite joints that were sheared three times under 1 and 7 MPa of normal stress, respectively, are described below.

The shear stress is plotted against the shear displacement for the two joints that underwent three shearing events in

Fig. 17 Images of the three different infillings before and after shearing (from left to right: dry soil, wet soil and cement mortar particles). The same normal stress (3 MPa) was applied in each case, and the three joints that were used had planar surfaces



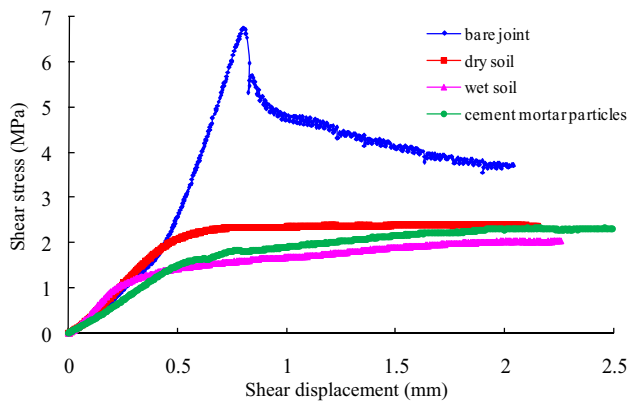


Fig. 18 Curves of shear stress vs. shear displacement for joints without fillings and joints with three different infillings (the normal stress was 3 MPa)

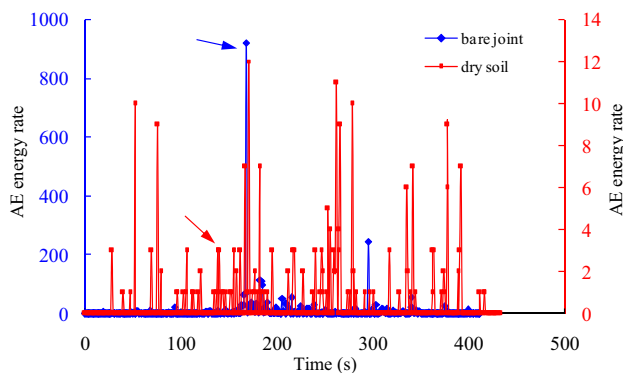
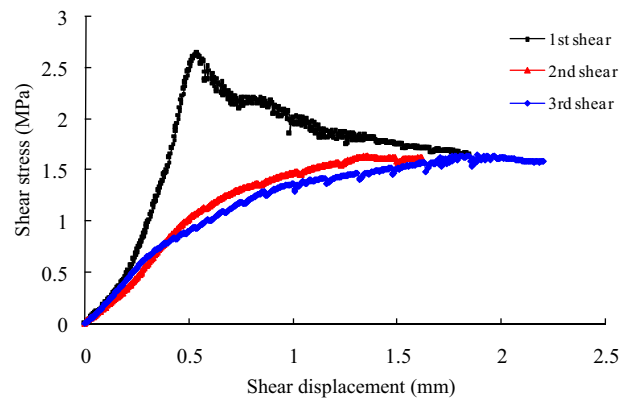


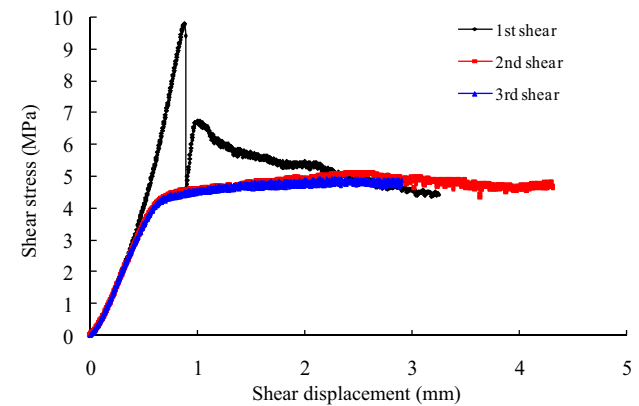
Fig. 19 Comparison of the energy rates from a joint with no filling and a joint that was filled with dry soil (left vertical axis in blue indicates the energy rate of the bare joint, and the right vertical axis in red represents the energy rate of the joint that was filled with dry soil; the blue and red arrows indicate the locations of the peak shear strength for the two joints)

Fig. 20a, b. As indicated in Fig. 20a, the peak shear strength decreased with the number of shear events. The strength for the second shearing was far below that of the first shearing, but only slightly higher than that of the third shearing, and the residual stress for the first shearing was approximately equal to the final stable stress values of the second and third shearings. Moreover, the shape of the stress curve for the first shearing was very different to the shape of the curves for the second and third shearings, and the sharp peak in the stress curve and the displacement weakening phenomenon disappeared after the second and third shearing events. The change in the shear stress with shear time for the granite joint was similar to that seen for the cement mortar joint, as shown in Fig. 20b. The strong post-peak shear stress drop vanished upon repeated shearing of the joint.

Based on the above analysis, the shear strength of a joint will decrease remarkably after the first shearing



(a)



(b)

Fig. 20 Shear stress and displacement curves for joints that experienced repeated shearing: **a** cement mortar joint; **b** marble joint

because of irreversible damage to the asperities. The residual strength of the first shearing was approximately equal to the strengths of the second and third shearings because the damage to the asperities had reached the limit under the same stress state. Because there was no post-peak shear stress drop or slip weakening of the shear stress after the first shearing, the energy released was lower when failure occurred, and the probability of rockbursts was lower.

The role of shear history in the mechanical behaviour of joints and rockbursts is very similar to that of infillings: both factors decrease the energy liberated and lower the risk of rockbursts. Fillings cover or protect asperities with infillings from damage, and previous shearings (i.e. a shear history) result in the destruction of prominent asperities and the clearance of obstacles to the next shearing. However, in the above discussion we assumed that the normal stress remained constant. If the normal stress increases, then the properties of the joint may change; for example, the shear strength may increase and more energy may be released at the point of failure.

Discussion

The shear failure of rock masses along a weak plane is one of the most common failure modes of the rock surrounding underground tunnels, and the above analysis indicates that both static shear failure and dynamic shear failure (rockbursts) occur in hard, brittle rock masses under high-geostress conditions. As rockbursts are violent events that manifest as the ejection of rock from excavation walls—often at high velocity, the support design and the support strategy applied under dynamic loading differ markedly from those needed when static shear failure occurs, and the reinforcing elements should yield and absorb energy under violent load impulses. By combining the actual geological conditions (such as the stress magnitude, rock types and joint surface characteristics) with the conclusions that were obtained in this study, we can predict the type of shear failure that is most likely to occur. Thus, targeted support systems can be designed and used accordingly, the efficiency of the support can be improved, and the cost can be minimized.

In addition to the gravitational stress and secondary stress caused by excavation, regional tectonic stress tends to build up around structural planes, which facilitates the occurrence of slip rockbursts. From the experiments performed in the present research, we know that if brittle and violent shear failure occurs, the shear stress drop may lead to rockbursts because of the large amount of energy released. However, rockbursts may also be induced in the wall rock of tunnels in less brittle and hard rock when weak planes are sheared in a slow manner, as this squeezes the rock and concentrates stress due to the movement of the discontinuity.

The compressive strength of a rock sample increases with the loading rate, and the rock will fail much more violently at a higher loading rate (Zhao 2000). The effect of the shear rate on fault slip rockbursts is not discussed in this study but remains important. When the shear rate is low, shear creep deformation may occur and the risk of rockbursts may be low; however, when the shear rate is high, such as during the conditions associated with blasting and earthquakes, joints may show different shear behaviour. Thus, it is very important to determine the effect of shear rate on fault slip bursts, so this topic requires further study.

For soft rock, small asperities on the joint surface are easily sheared off because of the low strength, and large asperities will experience ductile deformation and the energy will be dissipated immediately. Thus, energy cannot accumulate, and the risk of rockbursts from weak plane shearing is low. As with strain bursts, the properties of the rock also influence the occurrence of slip bursts. Energy is much more easily built up in brittle and hard rocks that are very strong, and rockbursts may occur when shear failure occurs in such cases.

In this study, only three simple and easily acquired infillings were used in the cement mortar joint shear tests, and the mechanical characteristics of a joint in a different host rock that is filled with the same material might differ, particularly when the normal stress is extremely high. Moreover, stick slip may occur when a fault is filled with silicate minerals from seismological research, and earthquakes may be induced (Summers and Byerlee 1977). Whether unstable slip will occur when the joint contains silicate minerals also requires further research. However, the normal stress applied in earthquake engineering research is up to several hundred MPa, in order to simulate the stress environment in the deep crust, which is much higher than the stress state in civil engineering tunnels. Thus, joints or faults may behave differently if the normal stress varies greatly, even for the same infilling and host rock. More exhaustive experiments should be designed that apply actual stress conditions and types of infillings so that the influence of different fillings on slip rockbursts in deep tunnels can be examined.

Conclusions

While there have been many studies of the factors that determine and influence strain bursts, which primarily occur in intact surrounding rock and are caused by compression stress, only minor research effort has been directed into addressing rockbursts that are triggered by shear failure along discontinuities, such as structural planes, under high-geostress conditions. To determine the factors that influence fault slip rockbursts in deeply buried hard rock tunnels, shear tests were conducted on artificial splitting marble, granite and cement mortar joints under CNL conditions and various normal stresses. The shear behaviour and acoustic emission characteristics of these systems were studied, and the influences of rock type, normal stress, surface morphology, infilling, and shear history on fault slip rockbursts were systemically analysed and discussed. The following primary conclusions were drawn from these investigations:

1. Rockbursts occurred more readily when the granite joints were sheared because of either violent stress drops after the peak stress or stress drops during the stick-slip period due to the release of large amounts of energy. The plane where shear failure occurred either coincided with the damage site of the burst or was separate from the burst site and was the seismic focus. Moreover, rockbursts could occur repeatedly if unstable stick slip appeared. Static shear failure dominated for most of the marble and cement mortar joints, indicating a low risk of fault slip rockbursts.

2. The value of the stress drop immediately after the peak stress and the average stress drop during stick slip both increased with the normal stress; as stress drops were usually accompanied by the release of a large amount of energy, the probability and intensity of fault slip rockbursts increased with the normal stress. The failure mode and pattern of the joints were strongly influenced by the normal stress level. Under low normal stress, the joints were unbroken except for slight abrasion on the surface. With increasing normal stress, the front end of the hanging wall was impacted and fractured. As the normal stress was increased further, macrotensile fractures were generated in the footwall and hanging wall of the joint.
3. The shear behaviour was greatly affected by the surface morphology of the joint. The shear strength increased and a violent post-peak stress drop could occur if the surface was extremely rough, and tensile failure of the footwall initiated from valleys between high and large asperities was generated earlier than expected. Moreover, more intense shear rupture bursts could occur as intact rock was sheared off if the actual shear plane deviated from the pre-designed surface.
4. Infillings and previous shearing events (i.e. a shear history) reduced the peak shear strength of the joints, and the shear stress did not decrease with shear displacement after the peak stress (slip weakening disappeared); thus, the probability of fault slip rockbursts may decrease significantly because of the low amount of energy released.

The conclusions obtained in this study can be used to evaluate the fault slip rockburst potential during the construction of a deeply buried hard rock tunnel. For example, when the structural planes in the tunnel are filled with infillings, the risk of fault slip rockbursts is very low. When the tunnel is excavated in a granite rockmass, the rock is prone to fault slip rockbursts when the stress level is high, regardless of whether the joint surface is rough or planar.

Acknowledgments Financial support from the National Program on Key Basic Research Project of China under grant no. 2014CB046902 and from the National Natural Science Foundation of China under grant nos. 51279201, 41172288, 41472270 and 41372298 is gratefully acknowledged. The work in this paper was also supported by the Open Research Fund of State Key Laboratory of Geomechanics and Geotechnical Engineering, Institute of Rock and Soil Mechanics, Chinese Academy of Sciences (grant no. Z015007).

References

- Alber M (2013) Strength of faults—a concern for mining engineers. In: Kwasniewski M, Lydzba L (eds) Eurock. Taylor and Francis, London, pp 545–550
- Cai W, Dou LM, Gong SY, Li ZL, Yuan SS (2015) Quantitative analysis of seismic velocity tomography in rock burst hazard assessment. *Nat Hazards* 75(3):2453–2465
- Castro LAM, Carter TG, Lightfoot N (2009) Investigating factors influencing fault-slip in seismically active structures. In: Proc 3rd CAN-US Rock Mech Symp, Toronto, Canada, 9–14 May 2013, pp 1–12
- Chen GQ, Li TB, Zhang GF, Yin HY, Zhang H (2014) Temperature effect of rock burst for hard rock in deep-buried tunnel. *Nat Hazards* 72(2):915–926
- Cook NGW (1965) A note on rockbursts considered as a problem of stability. *J S Afr Inst Min Metall* 65(3):437–446
- Durrheim J, Roberts MKC, Haile AT, Hagan TO, Jager AJ, Handley MF, Spottiswoode SM, Ortlepp WD (1998) Factors influencing the severity of rockburst damage in South African gold mines. *J S Afr Inst Min Metall* 98(3/4):53–57
- Feng XT, Chen BR, Zhang CQ et al (2013) Mechanism, warning, and dynamic control of rockburst development processes. Science Press, Beijing (in Chinese)
- Hasegawa HS, Wetmiller RJ, Gendzwill DJ (1989) Induced seismicity in mines in Canada—an overview. *Pure Appl Geophys* 129(3–4):423–453
- He MC, Xia HM, Jia XN, Gong WL, Zhao F, Liang KY (2012a) Studies on classification, criteria and control of rockbursts. *J Rock Mech Geotech Eng* 4:97–114
- He MC, Nie W, Zhao ZY, Guo W (2012b) Experimental investigation of bedding plane orientation on the rockburst behavior of sandstone. *Rock Mech Rock Eng* 45:311–326
- Hofmann GF, Scheepers LJ (2011) Simulating fault slip areas of mining induced seismic tremors using static boundary element numerical modelling. *Min Technol* 120(1):53–64
- Huang BX, Liu JW (2013) The effect of loading rate on the behavior of samples composed of coal and rock. *Int J Rock Mech Min Sci* 61:23–30
- Kaiser PK, Cai M (2012) Design of rock support system under rockburst condition. *J Rock Mech Geotech Eng* 4(3):215–227
- Kaiser PK, McCreath DR, Tannant DD (1996) Canadian rockburst support handbook. CAMIRO, Sudbury
- Linkov AM (1996) Rockburst and the instability of rock masses. *Int J Rock Mech Min Sci Geomech Abstr* 33:727–732
- Liu ZB, Shao JF, Xu WY, Meng YD (2013) Prediction of rock burst classification using the technique of cloud models with attribution weight. *Nat Hazards* 68(2):549–568
- Meng FZ, Zhou H, Wang ZQ et al (2016) Experimental study on the prediction of rockburst hazards induced by dynamic structural plane shearing in deeply buried hard rock tunnels. *Int J Rock Mech Min Sci* 86:210–223
- Morrison DM (1989) Rockburst research at Falconbridge's Strathcona Mine, Sudbury, Canada. *Pure Appl Geophys* 129(3–4):619–645
- Ortlepp WD (2000a) Study of rockburst source mechanism. Safety in Mines Research Advisory Committee, GAP 524. Steffen, Robertson and Kirsten, Vancouver, pp 1–42
- Ortlepp WD (2000b) Observation of mining-induced faults in an intact rock mass at depth. *Int J Rock Mech Min Sci* 37(1):423–436
- Ortlepp WD (2005) RaSiM comes of age: a review of the contribution to the understanding and control of mine rockbursts. In: Potvin Y, Hudyma M (eds) Proceedings of the Sixth International Symposium on Rockburst and Seismicity in Mines. Australian Centre for Geomechanics, Perth, pp 3–20
- Ortlepp WD, Stacey TR (1994) Rockburst mechanisms in tunnels and shafts. *Tunn Undergr Space Technol* 9:59–65
- Ryder JA (1988) Excess shear stress in the assessment of geologically hazardous situations. *J S Afr Inst Min Metall* 88(1):27–39
- Sainoki A, Mitri HS (2014a) Dynamic behaviour of mining-induced fault slip. *Int J Rock Mech Min Sci* 66:19–29

- Sainoki A, Mitri HS (2014b) Dynamic modelling of fault slip with Barton's shear strength model. *Int J Rock Mech Min Sci* 67:155–163
- Sainoki A, Mitri HS (2015) Effect of slip-weakening distance on selected seismic source parameters of mining-induced fault-slip. *Int J Rock Mech Min Sci* 73:115–122
- Simon R (1999) Analysis of fault-slip mechanisms in hard rock mining. PhD thesis. Department of Mining and Metallurgical Engineering, McGill University, Montreal
- Stacey TR (2011) Support of excavations subjected to dynamic (rockburst) loading. In: *Proc 12th Int Congr Int Soc Rock Mech*, Beijing, China, 16–21 Oct 2011, pp 137–145
- Summers R, Byerlee JA (1977) A note on the effect of fault gouge composition on the stability of frictional sliding. *Int J Rock Mech Min Sci Geomech Abstr* 14(3):155–160
- Swanson PL (1992) Mining-induced seismicity in faulted geologic structures: an analysis of seismicity-induced slip potential. *Pure Appl Geophys* 139(3–4):657–676
- Vatcher JL (2012) Architecture of a classification system to evaluate fault slip risk in a mining environment. Master thesis. The Robert M. Buchan Department of Mining, Queen's University, Kingston
- White BG, Whyatt JK (1999) Role of fault slip on mechanisms of rock burst damage, Lucky Friday Mine, Idaho, USA. In: *Proc 2nd Southern African Rock Eng Symp: Implementing Rock Engineering Knowledge*, Johannesburg, S. Africa, 13–15 Sept 1999, pp 1–10
- Zhang CQ, Feng XT, Zhou H, Qiu SL, Wu WP (2012) Case histories of four extremely intense rockbursts in deep tunnels. *Rock Mech Rock Eng* 45:275–288
- Zhao J (2000) Applicability of Mohr–Coulomb and Hoek–Brown strength criteria to the dynamic strength of brittle rock. *Int J Rock Mech Min Sci* 37(7):1115–1121
- Zhao XG, Cai M (2015) Influence of specimen height-to-width ratio on the strainburst characteristics of Tianhu granite under true-triaxial unloading conditions. *Can Geotech J* 52:1–13
- Zhao XG, Wang J, Cai M, Cheng C, Ma LK, Su R, Zhao F, Li DJ (2014) Influence of unloading rate on the strainburst characteristics of Beishan granite under true-triaxial unloading conditions. *Rock Mech Rock Eng* 47:467–483
- Zhou H, Meng FZ, Zhang CQ et al (2015) Analysis of rockburst mechanisms induced by structural planes in deep tunnels. *Bull Eng Geol Environ* 74(4):1435–1451